RESEARCH ARTICLE

Candle soot nanoparticle embedded nanofibrous membrane for separation of miscible and immiscible oil/water mixtures

Kamala Thota[1] | Kiran Donthula[1] | Chandra Shekhar[2] | Ramsagar Vooradi[1] |
Manigandan Sabapathy[2] | Manohar Kakunuri[1]

[1]Department of Chemical Engineering, National Institute of Technology, Warangal, India

[2]Department of Chemical Engineering, Indian Institute of Technology Ropar, Rupnagar, Punjab, India

Correspondence
Manohar Kakunuri, Department of Chemical Engineering, National Institute of Technology, Warangal 506004, India.
Email: manohar@nitw.ac.in

Abstract

Candle soot (CS) nanoparticles exhibit excellent superhydrophobic and superoleophilic properties, making them an ideal absorbent for separating oil and oil/water mixtures. Although their cost-effectiveness is attractive, the challenges associated with recovering soot nanoparticles after oil absorption and producing secondary pollutants have limited their attention. Our study demonstrates the synthesis of CS nanoparticles embedded polystyrene (PS) nanofibrous membranes with excellent stability, surface-to-volume ratios, and flexibility. CS-incorporated composite membrane with a rough surface showed a water contact angle (WCA) of $156° ± 1.5°$, about 20% higher than the smooth pristine PS membrane. The CS-based composite membrane also demonstrated improved performance as an absorbent, owing to its hydrophobic characteristics linked with surface roughness when employed for separating oil from oil/water mixtures. Furthermore, when exposed to four different oils, the CS-based membrane displayed a higher absorption capacity (up to ≈ 120 g oil/g membrane) than the pristine membrane. Using a gravity-assisted continuous oil/water separation setup, we measured the oil permeate flux using nanofiber mats as a membrane. Compared to the original membrane, the modified membrane showed enhanced oil permeate flux of $\sim 2873 ± 122$ L m^{-2} h^{-1} and separation efficiency of over 99%.

KEYWORDS

candle soot, electrospinning, oil/water separation, superhydrophobicity, superoleophilicity

1 | INTRODUCTION

Over the past few years, oil spills have been reported frequently in oceans and rivers. For instance, a massive accident in the Gulf of Mexico in 2010 dumped approximately 4.9 million barrels of oil into the sea.[1] Oil pollution, which has perpetually increased around the globe, also results from oily wastewater disposal from petrochemical, textile, metal, and food industries, etc.[2–5] Consequently, oil spills and oily substances from wastewater severely damage marine and aquatic ecosystems and coastal environments.[6] Various physical, chemical, and biological methods have been used to address oil recovery from oil/water mixtures.[7–12] Conventional methods (in situ burning, skimming, ultrasonic separation, chemical dispersion, etc.) have several demerits, such as generating secondary pollutants, low efficiency, high operating costs, low energy utilization, and poor reusability.[11–14] Membrane-based oil/water separation with profound absorption capacity is attractive among the numerous

oil/water separation techniques due to its excellent removal efficiency.[15–17] The ability of membrane materials with adjustable porosity and pore size distribution to separate miscible oil/water mixtures (emulsions) is an advantage over sponges and aerogels that have relatively large pores.[18,19] Furthermore, aerogels and sponge-based materials suffer from low absorption capacities, the inability to separate oil and water from miscible mixtures, and complex preparation methods. Various membranes are available for separating oil from oil/water mixtures, including oil-removing (superhydrophobic/ superoleophilic) or water-removing (superhydrophilic/ superoleophilic).[20–22] However, it is more economical to use the oil-removing type over the water-removing membrane since the extent of oil separation is relatively more straightforward than the large quantity of water from the given oil/water immiscible mixture.

In oil/water separation, the decontamination is usually accomplished via the following two routes: removing oil from (i) the immiscible oil/water mixtures and (ii) the miscible oil/water emulsions.[23,24] Several methods have been developed to separate oil from immiscible oil/water mixtures. However, separating oil from miscible oil/water emulsions is especially challenging since the mixtures are stable and the droplets are smaller than 20 μm.[25] Furthermore, the stabilized emulsions offer enhanced resistance to oil transport from the pores to the bulk. Therefore, it is imperative to devise a technique to remove oil traces from both immiscible and miscible oil/water mixtures.

There is a growing trend to use electrospun nanofiber membranes to deal with oil contamination.[26–30] The increase in interest in nanofiber-based membranes may be attributed to the ability of the membranes to separate oil from miscible and immiscible oil/water mixtures because of their tunable porosity, physicochemical properties that can be adjusted, flexibility, and large surface area.[28,31,32] Several electrospun nanofibrous membranes were prepared using polyvinylidene fluoride (PVDF), PS, polyacrylonitrile (PAN), poly(vinyl alcohol) (PVA), and agar/PVA for the separation of oil and water mixtures.[33–37] These nanofibers, however, showed poor efficiency, low mechanical strength, and low WCA values (< 150°).[23] In order to enhance WCA, porosity, surface area, and absorption capacity, various nanoparticles such as Fe_2O_3, SiO_2, Fe_3O_4, and TiO_2 were added into the polymer precursor before electrospinning to obtain the composite nanofibers.[34,38,39] These composites displayed considerable performance due to their higher WCA, good chemical resistance, and high hydraulic stability compared to other polymer-based pristine membranes. Recently, CS nanoparticles were also demonstrated to be an active material for different applications due to their uniform particle size of between 30 and 50 nm, ease of synthesis, and low cost.[40]

These soot particles displayed superhydrophobic and super-oleophilic properties owing to their low surface energy hydrocarbon and methyl functional groups.[41,42] Although these soot particles showed remarkable properties, their poor adhesion and difficulty in recovery hinder the use of these particles for oil/water separation. One way to overcome these challenges could be depositing CS particles on paraffin wax, polydimethylsiloxane, methyltriethoxysilane-based surfaces or combining the same with a polymer solution before electrospinning to fabricate stable superhydrophobic surfaces.[43–47] In several studies, stable superhydrophobic surfaces have been obtained using CS nanoparticles. However, these materials have not been evaluated as oil/water separation absorbents. The soot-embedded polyvinylidene fluoride (PVDF) nanofibrous membrane,[47] CS-coated nickel foam,[48] copper mesh,[10] melamine sponge,[49] and egg carton materials[50] are examples. However, CS particles have fragile adhesion to substrate materials in most cases, which must be addressed to make them robust and reusable for oil/water separation.

To this end, we propose demonstrating the oil/water separation using a CS-PS nanofiber-based composite membrane. The proposed strategy combines the synergistic effect of superhydrophobicity and three-dimensional complex channels to offer a novel yet straightforward membrane with improved flexibility, porous structure, and stability. Although several studies have been reported on PS-based nanofibers, no studies on soot-incorporated PS nanofibers are found in the literature. To the best of our knowledge, it is the first time that a membrane modified with soot particles has been used to demonstrate the removal of oil from immiscible oil/water mixtures and miscible oil/water emulsions.

2 | METHODOLOGY

2.1 | Materials

Polystyrene, Mw: 350,000 g/mol, purchased from Sigma-Aldrich Chemicals Pvt. Ltd., India, was used to prepare nanofibers. *N,N*-Dimethylformamide (DMF), and tetrahydrofuran (THF), used to dissolve PS in a suitable volume ratio, were purchased from Sigma-Aldrich Chemicals Pvt. Ltd., India. The non-aqueous phase-based absorbate (Peanut oil, bean oil, sunflower oil, and diesel), used to measure membrane oil absorption capacity, was procured from Taranath Scientific & Chemical, India. Span 80, an emulsifier, was purchased from SRL chemicals, India. The paraffin-based candle, procured from Taranath chemicals, India, has been used in preparing the soot particles. The coloring agents, methylene blue and Sudan IV, purchased from HIMEDIA chemicals, were used to stain water and oil phases. Deionized water (18.2 MΩ) obtained from a Milli-
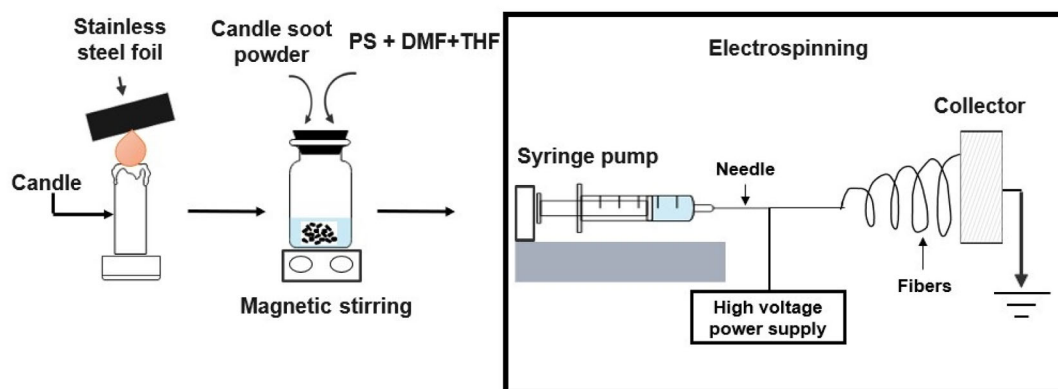
FIGURE 1 Illustration of the preparation methodology of the CS-incorporated PS nanofiber-based composite membrane.

Q™ was used for all experiments that involved aqueous phases. All the chemicals and the reagents were utilized as received without further purification.

2.2 | Preparation of superhydrophobic/superoleophilic surface

Figure 1 shows the schematic of the membrane synthesis process using electrospinning. First, CS was deposited uniformly on the stainless-steel foil by directing the soot flame straight into the substrate. The deposited CS particles were scraped off the foil and dried at 200°C for an hour inside the vacuum oven to remove wax content; this step is essential to prevent soot particle agglomeration during solution preparation. In a separate set of experiments, we prepared the polymer solution by dissolving 15 wt% of PS in a binary solvent mixture containing DMF and THF solvents at a ratio of 4:1 (by volume). The precursor solution was then gradually introduced with 10 wt% soot particles in powder form. In order to achieve a uniform solution, a magnetic stirrer was used to stir the mixture at 300 RPM for 8 h. The obtained PS solution containing CS was used as a precursor to electrospinning. Under 45% relative humidity and room temperature conditions, the electrospinning process parameters such as voltage, flow rate, and needle-to-rotating drum collector (RPM: 300) distance were optimized as 15 kV, 0.8 mL/h, and 10 cm, respectively. We used a 5-mL syringe fitted with an 18-gauge needle for discharging the polymer solution. The fibers deposited over the drum for 6.5 h were removed as a mat and used as an absorbent.

2.3 | Oil absorption

We conducted a series of experiments to gauge the performance of the membrane. In a separate set of experiments, four different oils (peanut oil, sunflower oil, diesel oil, and

bean oil) were considered to determine the absorption capacity of the as-synthesized PS and CS-PS nanofiber-based membrane. We placed membranes weighing about 0.1 g in a beaker containing oil and allowed them to absorb oil. The membranes reached equilibrium and showed a sluggish increase in the absorption capacity, as shown in Figure S1. Hence the absorption time was maintained as 2 min in absorption studies. The absorption capacity was then calculated using the following expression.

$$\text{Absorption capacity} = \frac{M_2 - M_1}{M_1} \qquad (1)$$

In the equation above, M_1 and M_2 refer to the mass of the membrane before and after absorption, respectively.

2.4 | Oil/water separation

2.4.1 | Immiscible oil/water system

We conducted a series of experiments with PS and CS-PS membranes to determine the separation efficiency and permeate flux. For the study, we first prepared an immiscible oil/water mixture using sunflower oil and water in a volume ratio of 1:1 (25 mL each). We stained the water and oil phase using methylene blue and Sudan IV to visualize the aqueous and oil phase. The mixture was then slowly poured into a lab-scale oil/water separation setup, where liquid passes through a membrane and collects in a flask below, as shown in Figure S3. Oil flowed through the membrane solely by gravity, without the aid of any external forces.

2.4.2 | Miscible oil/water system

In the case of the emulsion mixture, we performed the study using the stabilized oil dispersed in the form of

droplets in the aqueous phase. Initially, 1 mL of water was added to 50 mL of sunflower oil containing 0.1 g of surfactant (Span 80). Subsequently, the entire oil/water mixture was vigorously stirred for 3 h at 1200 RPM to obtain oil/water emulsion. After that, the oil/water separation was performed following a similar procedure described in the immiscible oil/water separation mentioned earlier. Before emulsification, we stained the aqueous phase using methylene blue to visualize the aqueous and oil phase. As mentioned in the earlier section, no additional forces were introduced to improve the flux. The ratio of the volumetric flow rate (L/h) of the oil collected at the bottom using gravity-assisted separation and the membrane's effective surface area is reported as the membrane permeate flux. In addition, a separation efficiency calculation was performed based on the equation below for both immiscible and emulsified oil/water mixture separation.

$$\text{Separation efficiency}(\%) = \frac{\text{Amount of oil removed via separation}}{\text{Total amount of oil added}} \times 100\% \quad (2)$$

2.5 | Characterization

High-resolution scanning electron microscope (HRSEM; Carl Zeiss, EVO 18), studies were performed to characterize the CS-laden PS nanofibers. The membrane's WCA measurement has been realized through the sessile drop experiments using the optical tensiometer (Biolin Scientific, Theta Flex) under static mode. The WCA of each sample has been obtained by capturing the images at several locations in X and Y planes using the optical tensiometer and then averaging the measured values obtained at different spatial coordinates. Fourier transform infrared (FTIR) spectroscopy (Thermo Scientific Nicolet, iS50) was used to identify the functional groups of the pristine and composite membrane and confirm the presence of CS nanoparticles. A thermogravimetric analysis (TGA) and derivative thermogravimetric analysis (DTA) were conducted with the TGA instrument (SDT650) to investigate the thermal stability of CS-incorporated and pristine PS nanofiber membranes.

3 | RESULTS AND DISCUSSION

First, we examined the structural morphology of CS incorporated and pristine PS nanofiber membrane by obtaining a three-dimensional projection of surface features using SEM. Figure 2A–C depicts the scanning electron microscopic images corresponding to the modified

PS membrane, while the pristine nanofiber membrane's surface morphology is distinctly shown in Figure 2E–G. As illustrated by Figure 2C, the surface of nanofiber modified by soot particles appears to have a significant level of roughness compared to the smooth pristine nanofibers (Figure 2G). Consequently, it is expected to enhance the wettability nature demonstrated by the surface's nano-/microscale features, that is, hydrophobicity in this case.[51] The nanoscale surface features in CS mixed fibers are attributed to the rippled structures distended from the surface, which resulted from incorporating the soot nanoparticles in the matrix of PS nanofibers. The changes in the surface morphology of composite membranes can be attributed to the difference in the evaporation rates of solvent-rich PS and solvent-less CS during the whipping of fibers between needle and collector, which leads to shrinkage of the nanofibers. Unlike other soot-based superhydrophobic membranes that have been reported, these nanofibers do not just have soot particles sitting on the surface. Instead, the soot particles are spread out throughout the polymer matrix.[46–49] On the other hand, the uniform evaporation rate in the case of pristine PS nanofibers leads to smooth surface morphology, as shown in Figure 2E–G.

The wettability of the membrane plays a crucial role in oil recovery application. To this end, we demonstrate the influence of surface roughness on the wettability of the membrane. Figure 2D,H reveals the WCA of a droplet deposited on the surface of a modified and pristine PS membrane. The average WCA of CS incorporated and pristine PS nanofibers measured by the sessile drop studies are $156° \pm 1.5°$ and $129° \pm 1°$, respectively. We infer that the modified nanofiber mat shows an improvement in WCA of $27°$, that is, an increase of up to 21%, compared to the pristine PS nanofiber membrane. This enhancement in WCA (hydrophobic to superhydrophobic) signifies the substantial role of nano-/microscale surface roughness coupled with a reduction in surface energy tuned by the proposed CS–PS matrix.

The molecular vibrations of functional groups in CS-incorporated PS and pristine PS nanofibers were investigated using FTIR spectra. Figure 3 shows the FTIR spectrum of pristine and CS-incorporated PS membranes. The appearance of characteristic peaks at three different regions, (1) 400–900 cm^{-1}, (2) 900–2000 cm^{-1}, and (3) 2800–3200 cm^{-1}, establish the existence of the unique chemical composition of PS. Aromatic rings with C—H band vibrations exhibit peaks at 759 and 690 cm^{-1}. Peaks at 1584 and 1030 cm^{-1}, lying between 900 and 2000 cm^{-1}, indicate aromatic deformation of C—C and C—H bonds. The peak at 2916 cm^{-1} corresponds to the C—H stretching vibration of the CH$_2$ and CH groups.[52] On the other hand, the strong peaks observed at 3694
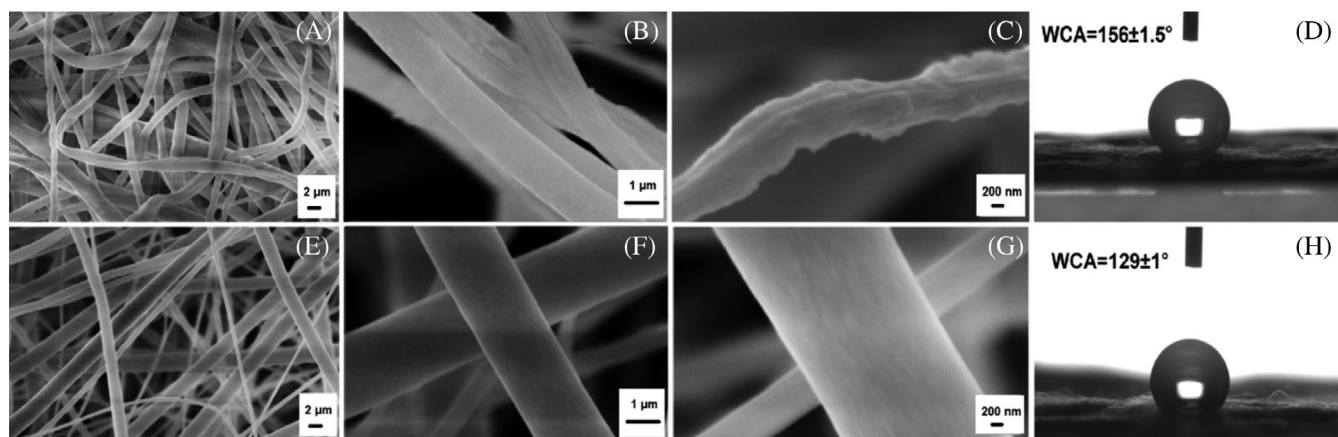
FIGURE 2 The representative SEM images: (A–C) CS incorporated PS nanofibers at different magnifications; (E–G) Pristine PS nanofibers at different magnifications; (D, H) WCA for CS incorporated PS and Pristine PS nanofibers, respectively.
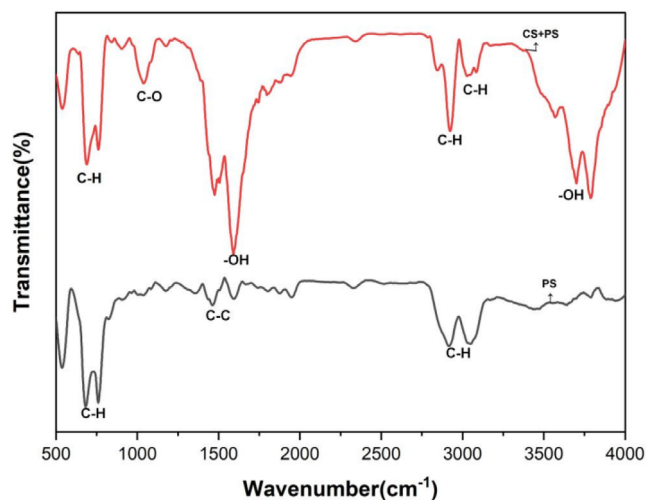

FIGURE 3 FTIR spectrum of CS incorporated PS and pristine PS nanofibers.

and 1587 cm^{-1} for CS-incorporated PS composite samples denote the existence of a hydroxyl group due to the profound stretching of the O—H bond due to the presence of the absorbed water phase.[40] Furthermore, we confirm the presence of the CS nanoparticles in the PS membrane by observing the characteristic peak for the carboxylic group at 1048 cm^{-1}.[53] Thus, the FTIR results discussed earlier clearly indicate that the composition of the modified membrane is different from pristine PS due to the incorporation of CS nanoparticles in the matrix.

Figure 4A,B shows the thermogravimetric analysis (TGA) and derivative thermogravimetry (DTG) curves of pristine PS and CS-incorporated PS nanofibers. The membrane samples were heated from room temperature to 800°C with a heating rate of 10°C/min. The TG analysis of both samples shows one-step degradation; however, the decomposition temperature of CS-incorporated PS fibers is

slightly higher than pristine PS fibers (i.e., ∼10°C) due to enhanced thermal stability. After degradation, the remaining weight (≈8 wt%) of the CS-embedded PS nanofiber membrane can be attributed to embedded CS nanoparticles in the composite nanofibers. DTG peak of maximum weight loss shifted to a higher temperature for CS-embedded PS nanofibers compared to pristine nanofibers, as shown in Figure 4B (inset). A rise in decomposition temperature can be attributed to the interaction between PS and CS, which inhibited the process.

Furthermore, we show that the performance of the modified membrane over the removal of oil from the oil/water mixtures is higher than the unmodified one. Figure S2a–c shows the snapshots of the glass beakers containing the oil/water mixtures with and without the addition of nanofiber-based absorbents. Figure S2b,c displays the pictures of the efficient removal of CS-modified PS absorbent at $t = 0$ (Figure S2b) and $t = 2$ min (Figure S2c). It can be inferred from the figures (Figure S2b,c) that the CS-incorporated PS nanofibers-based membrane has almost removed the absorbate (target pollutant). The oil phase is stained using Sudan IV to visualize the oil phase distinctly. Similar experiments were performed using a pristine PS nanofiber-based membrane to assert the efficiency in terms of oil separation. It is evident from the images shown in Figure S2a–f that the composite membrane absorbed the entire amount of oil in 2 min while the pristine PS membrane equal in weight exhibited a lesser absorption capacity in a given time.

Next, we present the absorption capacity of the pure and composite membranes based on four different oils. The change in density of these four oils is insignificant (see Table S1), and the viscosity is in the range of 4.75 mPa s (diesel) to 78.45 mPa s (peanut oil). The plot depicting the absorption capacity based on different types
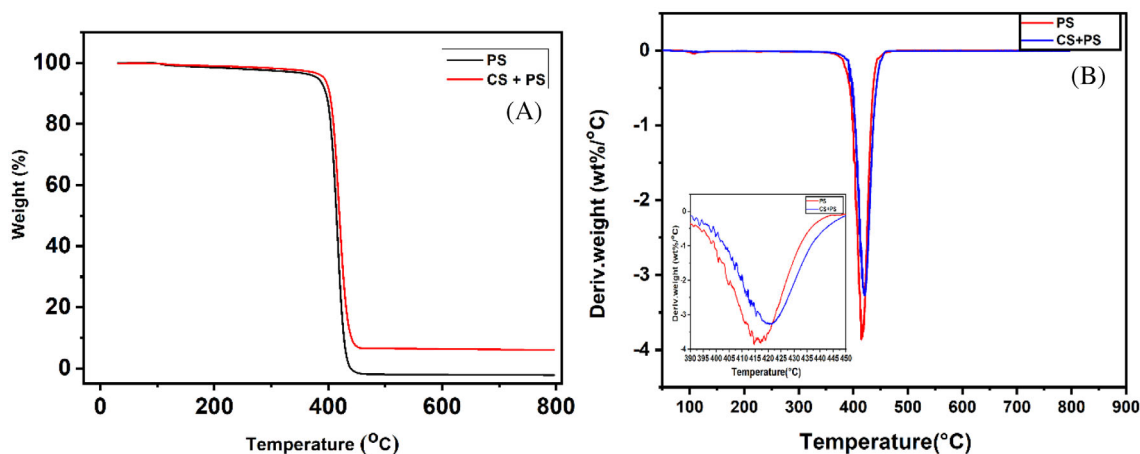
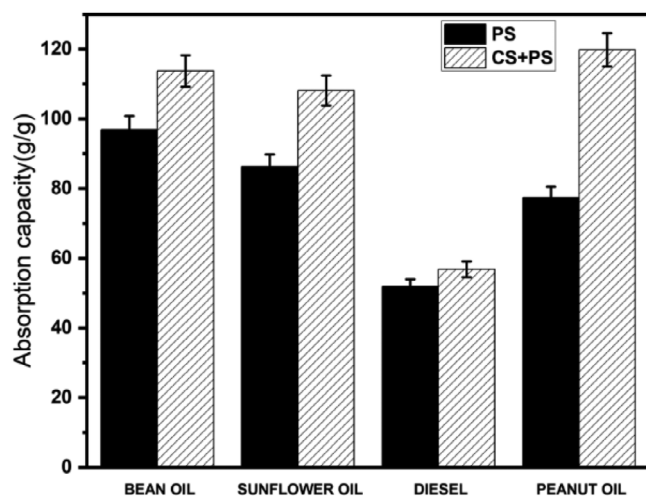**FIGURE 4** (A) TGA and (B) DTG curves of CS incorporated PS (CS+PS) & pristine PS nanofiber membranes.

FIGURE 5 Plot showing the pristine and composite membrane performance based on different types of oil.

of oil is shown in Figure 5. We infer from the bar graph (Figure 5) that the performance of the composite membrane is better than the pristine PS membrane in terms of absorption capacity, irrespective of any oil type. The sorption capacities of CS-incorporated PS nanofibers-based sorbent performed over four different types of oil are 119.78 (peanut), 113 (bean), 108 (sunflower), and 56 (diesel) g/g. On the contrary, we found the performance of pristine PS membrane absorption capacity to be lowest irrespective of any oil. The oil sorption capacity is also related to viscosity; the oil sorption capacity increases as viscosity increases. This could be due to higher resistance to the flow of oil in the entangled nanofibrous structure for high-viscosity oils.

The sorption capacities of pure PS membrane based on four different oil types achieved, in descending order, are 96 (bean), 86 (sunflower), 77 (peanut), and 50 (diesel) g/g. A tremendous increase is found in the composite

membrane when applied to a specific type of oil. For instance, we found a maximum of 154% increase in sorption capacity for the composite membrane when performed to separate peanut oil from the mixture. This exceptional performance of the CS-modified membrane may be ascribed to the enhanced WCA and nano/micro-scale surface roughness induced by the CS particles in the matrix of PS nanofibers. The reusability of the membrane was conducted for the CS-embedded membrane. The separation efficiency reduced significantly with the number of cycles, as depicted in Figure S4.

Following the absorption studies, we determined the oil-permeability of composite and pristine membranes based on gravity-driven oil/water separation using the setup shown in Figure S3. The experiment involves admitting the oil/water mixture at one end and collecting the permeate at the other end through the membrane. Figure S3a,d (left) shows the initial state of the immiscible oil/water and homogeneous w/o emulsion mixture before separating. Furthermore, we examined how well the CS–PS composite membrane permeates excess oil in an extreme scenario where oil is present in large quantities compared to water by exposing the membrane to w/o emulsion instead of o/w. We found that the proposed composite membrane shows excellent oil permeability even when oil is in a large volume. The permeate flux studies revealed that CS-based composite membrane performance is relatively higher than the pristine PS membrane.

Figure S3c,f illustrates the process of separating oil from the immiscible and miscible (w/o emulsion) mixture. The permeability and separation efficiency of the composite membrane applied over an immiscible mixture were $2873 \pm 122 \, L \, m^{-2} \, h^{-1}$ and $99 \pm 0.1\%$, respectively. Likewise, the permeability of the CS–PS nanofiber-based membrane determined for the case of w/o emulsion was $1602 \pm 93 \, L \, m^{-2} \, h^{-1}$. In contrast, the permeability and
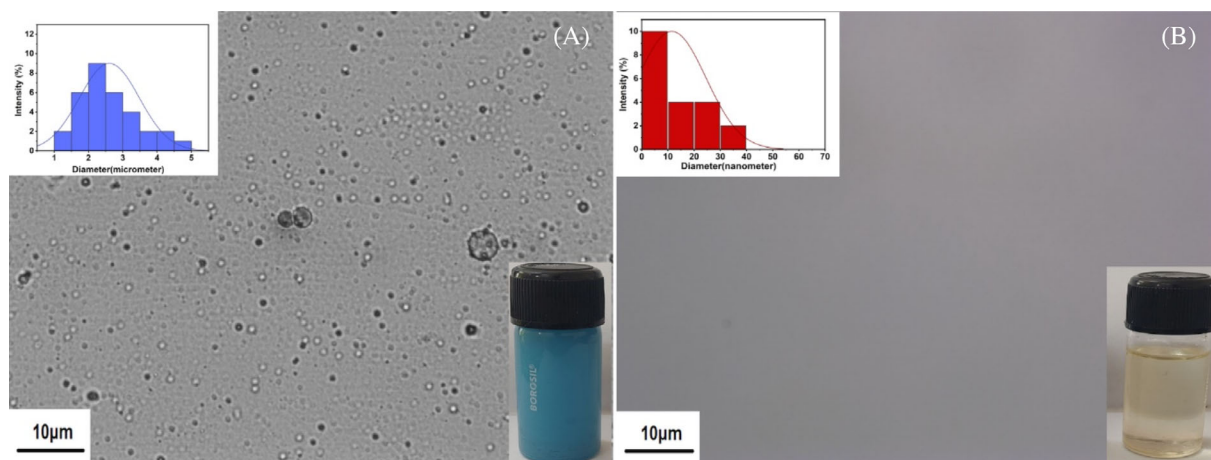
FIGURE 6 Optical microscopic images of w/o emulsion (A) before separation (B) after separation.

TABLE 1 Performance of different PS and its composite nanofiber-based membranes.

S.No.	Material	Oil absorption capacity (g/g)	WCA (°)	Reference
1	PS-SiO$_2$ composite micro/nanofiber	122.7	153	[39]
2	PVC/PS composite nanofibers	146	Not reported	[54]
23	PS/ Fe$_3$O$_4$ composite nanofibers	Not reported	162	[38]
4	PS/PAN composite nanofibers	194.85	144.32	[33]
40	PS on stainless steel mesh	Not reported	155	[55]
6	PS nanofibers	113	Not reported	[56]
7	PS/PU composite nanofibers	64.4	Not reported	[57]
8	CS incorporated PS nanofiber membrane	120	156	This work
9	Pristine PS nanofiber membrane	96.9	128	This work

separation efficiency of the pristine membrane found were $1262.62 \pm 89 \, \mathrm{L \, m^{-2} \, h^{-1}}$ and $85\% \pm 0.1\%$, respectively, which is significantly lower than the performance of the composite membrane in any mixture. The enhanced permeability of the composite membrane could be attributed to the high permeable membrane's increased superhydrophobicity and surface area. Figure 6A,B shows the optical images of w/o emulsion droplets stabilized by surfactant and the microgram of the resulting mixture after separation. Inset pictures of Figure 6A,B shows the particle size analysis of water in sunflower oil before and after the separation. It is clear from Figure 6 that the CS-incorporated electrospun PS membrane has entirely removed the emulsion droplets (dispersed phase).

Here, we present a comparison of the performance of various PS and its composite nanofiber membranes as an absorbent in oil/water separation applications. A comprehensive review of Table 1 indicates that the studies on permeate flux of immiscible oil based on the CS-modified PS nanofiber membrane have not been reported elsewhere. Although few studies were reported based on the Fe$_3$O$_4$-modified PS membrane,[23] absorption capacity is

significantly lower than CS-based composite membrane. We only looked at the performance of PS-based membranes to show how the PS–CS composite membranes we proposed in our work are better. The proposed study is the first of its kind. It is expected to provide various opportunities to develop new avenues under nanofiber-based membranes for water/oil separation.

4 | CONCLUSION

In summary, using a novel yet straightforward technique, we have fabricated a flexible CS-incorporated PS and pristine PS-based nanofiber membranes. The experimental results confirm that the oil absorption capacity, WCA, and permeate flux were significantly improved for CS-loaded PS-based membranes. The CS-incorporated nanofibers displayed a significant rise in WCA of $\mathbf{156° \pm 1.5°}$. This enhanced hydrophobicity promoted the affinity of the membrane towards oil and helped achieve a considerable permeate flux $\mathbf{(2873 \pm 122 \, L \, m^{-2} \, h^{-1})}$ with $\mathbf{99 \pm 0.1\%}$. We observed maximum absorption capacities in the case of soot-incorporated nanofibers-based PS

sorbent compared to pristine PS membrane. Furthermore, the as-prepared composite membrane displayed an excellent performance in applying the removal of emulsion droplets stabilized by surfactant with an excellent permittivity of $\mathbf{1602 \pm 93\,L\,m^{-2}\,h^{-1}}$. A detailed study is being done to figure out how the surface roughness depends on the concentration and type of CS particles. We believe that the proposed route will create a new avenue in dealing with oil/water separation using a soot-based composite membrane and provide ample opportunities for scientists to revisit interfacial science to explore further what is in store.

ACKNOWLEDGMENTS

CONFLICT OF INTEREST STATEMENT

There are no conflicts to declare.

DATA AVAILABILITY STATEMENT

Data available on request from the authors.

ORCID

Manigandan Sabapathy https://orcid.org/0000-0003-2250-8828
Manohar Kakunuri https://orcid.org/0000-0002-5825-0729

REFERENCES

1. Gray JL, Kanagy LK, Furlong ET, et al. Presence of the Corexit component dioctyl sodium sulfosuccinate in Gulf of Mexico waters after the 2010 Deepwater horizon oil spill. *Chemosphere*. 2014;95:124-130.
2. Wang X, Yu J, Sun G, Ding B. Electrospun nanofibrous materials: a versatile medium for effective oil/water separation. *Mater Today*. 2015;19:403-414.
3. Li Q, Kang C, Zhang C. Waste water produced from an oilfield and continuous treatment with an oil-degrading bacterium. *Process Biochem*. 2005;40:873-877.
4. Zerin I, Rasel Md. A case study on importance of salt recovery plant in textile dyeing industry. *Int J Ecotoxicol Ecobiol*. 2017;2:166-171.
5. Zheng Q, Li Z, Watanabe M. Production of solid fuels by hydrothermal treatment of wastes of biomass, plastic, and biomass/plastic mixtures: a review. *J Bioresour Bioprod*. 2022;7:221-244.
6. Luo J, Liu TL. Electrochemical valorization of lignin: status, challenges, and prospects. *J Bioresour Bioprod*. 2023;8:1-14.
7. Zhang X, Qu Q, Yang A, et al. Chitosan enhanced the stability and antibiofilm activity of self-propelled Prussian blue micromotor. *Carbohydr Polym*. 2023;299:120134.

8. Yong J, Huo J, Chen F, Yang Q, Hou X. Oil/water separation based on natural materials with super-wettability: recent advances. *Phys Chem Chem Phys*. 2018;20:25140-25163.
9. Saji VS. Wax-based artificial superhydrophobic surfaces and coatings. *Colloids Surfaces A: Physicochem Eng Asp*. 2020;602:125132.
10. Cao H, Fu J, Liu Y, Chen S. Facile design of superhydrophobic and superoleophilic copper mesh assisted by candle soot for oil water separation. *Colloids Surfaces A: Physicochem Eng Asp*. 2018;537:294-302.
11. Zhang J, Zhang F, Song J, et al. Electrospun flexible nanofibrous membranes for oil/water separation. *J Mater Chem A*. 2019;7:20075-20102.
12. Yeber M, Paul E, Soto C. Chemical and biological treatments to clean oily wastewater: optimization of the photocatalytic process using experimental design. *Desalin Water Treat*. 2012;47:295-299.
13. Sarbatly R, Krishnaiah D, Kamin Z. A review of polymer nanofibres by electrospinning and their application in oil–water separation for cleaning up marine oil spills. *Mar Pollut Bull*. 2016;106:8-16.
14. Liu W, Wu X, Liu S, Cheng X, Zhang C. CNT@LDH functionalized poly(lactic acid) membranes with super oil-water separation and real-time press sensing properties. *Polym Compos*. 2022;43:6548-6559.
15. Xiang B, Sun Q, Zhong Q, Peng M, Li J. Current research situation and future prospect of superwetting smart oil/water separation materials. *J Mater Chem A*. 2022;10:20190-20217.
16. Wu M, Xiang B, Mu P, Li J. Janus nanofibrous membrane with special micro-nanostructure for highly efficient separation of oil–water emulsion. *Sep Purif Technol*. 2022;297:121532.
17. Li H, Zhong Q, Sun Q, Xiang B, Li J. Upcycling waste pine nut Shell membrane for highly efficient separation of crude oil-in-water emulsion. *Langmuir*. 2022;38:3493-3500.
18. Duman O, Diker CO, Tunç S. Development of highly hydrophobic and superoleophilic fluoro organothiol-coated carbonized melamine sponge/rGO composite absorbent material for the efficient and selective absorption of oily substances from aqueous environments. *J Environ Chem Eng*. 2021;9:105093.
19. Duman O, Diker CO, Ugurlu H, Tunç S. Highly hydrophobic and superoleophilic agar/PVA aerogels for selective removal of oily substances from water. *Carbohydr Polym*. 2022;286:119275.
20. Liu L, Chen C, Yang S, Xie H, Gong MG, Xu X. Fabrication of superhydrophilic–underwater superoleophobic inorganic anticorrosive membranes for high-efficiency oil/water separation. *Phys Chem Chem Phys*. 2015;18:1317-1325.
21. Ma Q, Cheng H, Fane AG, Wang R, Zhang H. Recent development of advanced materials with special wettability for selective oil/water separation. *Small*. 2016;12:2186-2202.
22. Fan Q, Lu T, Deng Y, Zhang Y, Ma W, Xiong R. Bio-based materials with special wettability for oil-water separation. *Sep Purif Technol*. 2022;297:121445.
23. Zhang N, Yang X, Wang Y, et al. A review on oil/water emulsion separation membrane material. *J Environ Chem Eng*. 2022;10:107257.
24. Zhang Y, Zhao Y, Song B, et al. UV-fluorescence probe for detection Ni2+ with colorimetric/spectral dual-mode analysis method and its practical application. *Bioorg Chem*. 2021;114:105103.
25. Zhang J, Liu L, Si Y, Zhang S, Yu J. Tailoring electrospub nanofibrous materials for oil/water emulsion separation. *J Text Inst*. 2021;1:2285-2298.

26. Zong D, Zhang X, Yin X, et al. Electrospun fibrous sponges: principle, fabrication, and applications. *Adv Fiber Mater*. 2022; 4:1434-1462.

27. Zhou S, You T, Zhang X, Xu F, Appl ACS. Superhydrophobic cellulose nanofiber-assembled aerogels for highly efficient water-in-oil emulsions separation. *Nanostruct Mater*. 2018;1: 2095-2103.

28. Ma W, Zhang Q, Hua D, et al. Electrospun fibers for oil–water separation. *RSC Adv*. 2016;6:12868-12884.

29. Hou L, Wang N, Wu J, Cui Z, Jiang L, Zhao Y. Bioinspired Superwettability electrospun micro/nanofibers and their applications. *Adv Funct Mater*. 2018;28:1-22.

30. Deng Y, Lu T, Zhang X, et al. Multi-hierarchical nanofiber membrane with typical curved-ribbon structure fabricated by green electrospinning for efficient, breathable and sustainable air filtration. *J Membr Sci*. 2022;660:120857.

31. Liao Y, Loh CH, Tian M, Wang R, Fane AG. Progress in electrospun polymeric nanofibrous membranes for water treatment: fabrication, modification and applications. *Prog Polym Sci*. 2018;77:69-94.

32. Zhang Y, Zhao Y, Wu Y, et al. A biomass-derived Schiff base material composited with polylactic acid nanofiber membrane as selective fluorescent 'turn off/on' platform for Pb2+ quantitative detection and characterization. *Int J Biol Macromol*. 2022;214:414-425.

33. Li P, Qiao Y, Zhao L, et al. Electrospun PS/PAN fibers with improved mechanical property for removal of oil from water. *Mar Pollut Bull*. 2015;93:75-80.

34. Jiang S, Meng X, Chen B, Wang N, Chen G. Electrospinning superhydrophobic-superoleophilic PVDF-SiO$_2$ nanofibers membrane for oil-water separation. *J Appl Polym Sci*. 2020;137: 1-10.

35. Yang Y, Guo Z, Li Y, et al. Electrospun rough PVDF nanofibrous membranes via introducing fluorinated SiO$_2$ for efficient oil-water emulsions coalescence separation. *Colloids Surfaces A: Physicochem Eng Asp*. 2022;650:129646.

36. Duman O, Ugurlu H, Diker CO, Tunc S. Fabrication of highly hydrophobic or superhydrophobic electrospun PVA and agar/PVA membrane materials for efficient and selective oil/-water separation. *J Environ Chem Eng*. 2022;10:107405.

37. Sun F, Huang S, Ren H, et al. Core-sheath structured TiO$_2$@PVDF/PAN electrospun membranes for photocatalysis and oil-water separation. *J Polym Compos*. 2019;43:1.

38. Moatmed SM, Khedr MH, El-Dek SI, Kim HY, El-Deen AG. Highly efficient and reusable superhydrophobic/superoleophilic polystyrene@ Fe$_3$O$_4$ nanofiber membrane for high-performance oil/water separation. *J Environ Chem Eng*. 2019;7:103508.

39. Ding Y, Xu D, Shao H, Cong T, Hong X, Zhao H. Superhydrophobic-Superoleophilic SiO$_2$/polystyrene porous micro/nanofibers for efficient oil-water separation. *Fibers Polym*. 2019;20: 2017-2024.

40. Kakunuri M, Sharma CS. Candle soot derived fractal-like carbon nanoparticles network as high-rate lithium ion battery anode material. *Electrochim Acta*. 2015;180:353-359.

41. Liang CJ, Liao JD, Li AJ, et al. Relationship between wettabilities and chemical compositions of candle soots. *Fuel*. 2014;128: 422-427.

42. Mulay MR, Chauhan A, Patel S, Balakrishnan V, Halder A, Vaish R. Candle soot: journey from a pollutant to a functional material. *Carbon*. 2019;144:684-712.

43. Iqbal R, Majhy B, Sen AK, Appl ACS. Facile fabrication and characterization of a PDMS-derived candle soot coated stable biocompatible superhydrophobic and Superhemophobic surface. *Mater Interfaces*. 2017;9:31170-31180.

44. Deng X, Mammen L, Butt HJ, Vollmer D. Candle soot as a template for a transparent robust Superamphiphobic coating. *Science*. 2012;335:67-70.

45. Sutar RS, Latthe SS, Nagappan S, et al. Fabrication of robust self-cleaning superhydrophobic coating by deposition of polymer layer on candle soot surface. *J Appl Polym Sci*. 2021;138:1.

46. Seo K, Kim M, Kim DH. Candle-based process for creating a stable superhydrophobic surface. *Carbon*. 2014;68:583-596.

47. Lei T, Xiong J, Huang J, Zheng T, Cai X. Facile transformation of soot nanoparticles into nanoporous fibers via single-step electrospinning. *AIP Adv*. 2017;7:085212.

48. Zhao F, Liu LL, Ma F, Liu LL. Candle soot coated nickel foam for facile water and oil mixture separation. *RSC Adv*. 2014;4:7132-7135.

49. Gao Y, Zhou YS, Xiong W, et al. Highly efficient and recyclable carbon soot sponge for oil cleanup. *Mater Interfaces*. 2014;6:5924-5929.

50. Azad P, Raut S, Vaish R. Candle soot-coated egg carton material for oil water separation and detergent adsorption. *Bull Mater Sci*. 2020;43:2-7.

51. Bhushan B, Jung YC, Koch K. Micro-, nano- and hierarchical structures for superhydrophobicity, self-cleaning and low adhesion. *Philos Trans R Soc A Math Phys Eng Sci*. 2009;367:1631-1672.

52. Huang C, Niu H, Wu J, Ke Q, Mo X, Lin T. Needleless electrospinning of polystyrene fibers with an oriented surface line texture. *J Nanomater*. 2012;2012:1-7.

53. Yuan Z, Huang J, Peng C, et al. Facile preparation of superhydrophobic candle soot coating and its wettability under condensation. *Appl Phys A Mater Sci Process*. 2016;122:1.

54. Zhu H, Qiu S, Jiang W, Wu D, Zhang C. Evaluation of electrospun polyvinyl chloride/polystyrene fibers As sorbent materials for oil spill cleanup. *Environ Sci Technol*. 2011;45:4527-4531.

55. Lee MW, An S, Latthe SS, et al. Electrospun polystyrene nanofiber membrane with Superhydrophobicity and Superoleophilicity for selective separation of water and low viscous oil. *Mater Interfaces*. 2013;5:10597-10604.

56. Lin J, Shang Y, Ding B, Yang J, Yu J, Al-Deyab SS. Nanoporous polystyrene fibers for oil spill cleanup. *Mar Pollut Bull*. 2012;64:347-352.

57. Lin J, Tian F, Shang Y, et al. Co-axial electrospun polystyrene/polyurethane fibres for oil collection from water surface. *Nanoscale*. 2013;5:2745-2755.

SUPPORTING INFORMATION

Additional supporting information can be found online in the Supporting Information section at the end of this article.